

# Incorporating an allosteric regulatory site in an antibody through backbone design

Olga Khersonsky and Sarel J. Fleishman\*

Department of Biomolecular Sciences, Weizmann Institute of Science, Rehovot 76100, Israel

Received 30 October 2016; Accepted 24 January 2017

DOI: 10.1002/pro.3126

Published online 31 January 2017 proteinscience.org

**Abstract:** Allosteric regulation underlies living cells' ability to sense changes in nutrient and signaling-molecule concentrations, but the ability to computationally design allosteric regulation into non-allosteric proteins has been elusive. Allosteric-site design is complicated by the requirement to encode the relative stabilities of active and inactive conformations of the same protein in the presence and absence of both ligand and effector. To address this challenge, we used Rosetta to design the backbone of the flexible heavy-chain complementarity-determining region 3 (HCDR3), and used geometric matching and sequence optimization to place a Zn<sup>2+</sup>-coordination site in a fluorescein-binding antibody. We predicted that due to HCDR3's flexibility, the fluorescein-binding pocket would configure properly only upon Zn<sup>2+</sup> application. We found that regulation by Zn<sup>2+</sup> was reversible and sensitive to the divalent ion's identity, and came at the cost of reduced antibody stability and fluorescein-binding affinity. Fluorescein bound at an order of magnitude higher affinity in the presence of Zn<sup>2+</sup> than in its absence, and the increase in fluorescein affinity was due almost entirely to faster fluorescein on-rate, suggesting that Zn<sup>2+</sup> preorganized the antibody for fluorescein binding. Mutation analysis demonstrated the extreme sensitivity of Zn<sup>2+</sup> regulation on the atomic details in and around the metal-coordination site. The designed antibody could serve to study how allosteric regulation evolved from non-allosteric binding proteins, and suggests a way to designing molecular sensors for environmental and biomedical targets.

**Keywords:** allostery; protein design; antibody; metal binding; Rosetta; AbDesign

**Abbreviations:** EDTA, ethylenediaminetetraacetic acid; Fv, antibody variable fragment; HCDR3, heavy-chain complementarity-determining region 3; scFv, single-chain Fv; SPR, surface plasmon resonance

Additional Supporting Information may be found in the online version of this article.

**Statement:** Using backbone design in Rosetta, we designed a Zn<sup>2+</sup>-binding site into the variable domain of a fluorescein-binding antibody, so that the fluorescein-binding pocket would configure properly only upon Zn<sup>2+</sup> application. Regulation by Zn<sup>2+</sup> was reversible and sensitive to the divalent ion's identity, and came at the cost of stability and fluorescein-binding affinity. This strategy could be used to design molecular sensors for environmental and biomedical purposes.

Grant sponsors: European Research Council's Starter's Grant; Israel Science Foundation's Center for Research Excellence in Structural Cell Biology; Sam Switzer and Family.

\*Correspondence to: Sarel J. Fleishman, Department of Biomolecular Sciences, Ullman Building 301, Weizmann Institute of Science, Rehovot 76100, Israel. E-mail: sarel@weizmann.ac.il

## Introduction

All cells must sense changes in the concentrations of metabolites and signaling molecules to regulate their growth and development. At the molecular level, regulation is typically encoded by effector-molecule binding to an allosteric site in a protein (a site that is spatially distinct and nonoverlapping with the active site); effector binding must furthermore induce a conformational change in the active site, thereby modulating the protein's activity.<sup>1</sup> Recent experimental and theoretical work has suggested that allosteric regulation relies on the intrinsic flexibility observed to a different extent in all proteins, and the ability of effector binding or change in environmental conditions to shift the major conformational species between active and inactive (or partly active) states.<sup>2,3</sup>

Over the past decade, regulation was engineered and *in vitro* evolved,<sup>4</sup> for instance, by fusing naturally occurring binding domains to other binders and

enzymes,<sup>5–8</sup> by rational design of an active site for a model reaction into an already allosteric protein,<sup>9–11</sup> and by modifying the allosteric site's effector specificity.<sup>12</sup> Regulation was also demonstrated by “chemical rescue,” whereby an amino acid sidechain at the active site was eliminated, making activity conditional on binding of a mimic of the sidechain.<sup>13,14</sup> Despite these achievements, the design of an allosteric regulatory site into a protein through computational modeling has not been demonstrated. This design goal is moreover complicated because it requires design of different conformations with very similar free energies in the same protein. Computational protein design, by contrast, has focused almost exclusively on proteins with one stable conformation.<sup>15</sup>

To address this challenge, we decided to design an allosteric regulatory site into an antibody. Antibodies have several advantages for design of an allosteric site: foremost, antibodies are the most versatile class of binding molecules in nature, able to bind small molecules as well as large macromolecules with high affinity and specificity; the ability to design allosteric regulation in antibodies could therefore pave the way to design of allosteric binders in numerous cases. Second, there are >1,000 antibody structures in the Protein Data Bank (PDB), providing ample data on potential backbone conformations; and third, the antibody variable fragment (Fv) is modular, facilitating recombination of different backbones to generate diverse new conformations. Despite these important advantages, however, allosteric regulation is not known to occur in natural antibody variable fragments, and was not demonstrated by protein engineering, and therefore required a novel design strategy.

## Results

We chose the high-affinity fluorescein-binding antibody 4m5.3 (PDB entry: 1X9Q;  $K_D = 3 \times 10^{-13} \text{M}$ ) as a target for design,<sup>16</sup> and  $\text{Zn}^{2+}$  to serve as a positive effector. We set ourselves the goal to design new backbones in the most diverse heavy-chain complementarity-determining region HCDR3 that would be compatible with binding simultaneously to both  $\text{Zn}^{2+}$  and the native substrate fluorescein in spatially nonoverlapping sites. We predicted that in the absence of  $\text{Zn}^{2+}$ , the designed HCDR3 would be flexible and that application of  $\text{Zn}^{2+}$  would shift the Fv to the native fluorescein-binding conformation [Fig. 1(A)]. This design strategy therefore addresses the problem of designing effector sensitivity, but without the challenging problem of explicitly designing the inactive state and encoding the energy gap between inactive and active conformations in the presence and absence of ligand and effector.<sup>15,18,19</sup> Instead, our design strategy encodes favorable molecular contacts in the ligand- and effector-bound state only; it further assumes that introducing a  $\text{Zn}^{2+}$ -coordination

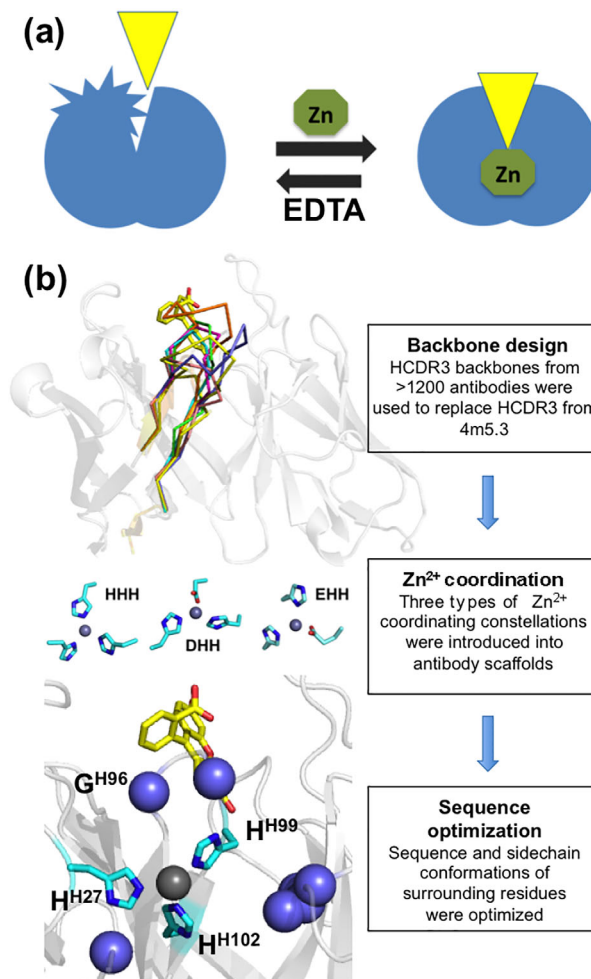


**Figure 1.** Overview of the algorithm for designing a  $\text{Zn}^{2+}$  regulatory site in antibody 4m5.3. A. Schematic of the design goal: in the absence of  $\text{Zn}^{2+}$  (left) HCDR3 is flexible (jagged lines), reducing binding of fluorescein (yellow wedge). Application of  $\text{Zn}^{2+}$  configures HCDR3, allowing fluorescein binding, whereas the metal-chelator EDTA reverses the effects of  $\text{Zn}^{2+}$ . B. Overview of the computational design workflow.  $\text{Zn}^{2+}$ -coordinating sidechains are shown as cyan sticks, fluorescein is shown in yellow sticks,  $\text{Zn}^{2+}$  as grey spheres and designed positions in and around HCDR3—as purple spheres. Residue numbering follows the Kabat convention for antibody variable domains.<sup>17</sup>

site in the conformationally flexible HCDR3 would destabilize the backbone in the absence of  $\text{Zn}^{2+}$  compared to the  $\text{Zn}^{2+}$ -bound state. This design strategy of positive-regulation through backbone preorganization has parallels in nature, for instance in the  $\text{Ca}^{2+}$ -modulated protein calmodulin.<sup>20</sup>

We started design calculations by using Rosetta *AbDesign*<sup>21</sup> to exchange the HCDR3 backbone of antibody 4m5.3 with the backbones of HCDR3s from >1,200 antibody structures obtained from the PDB [Fig. 1(B)]. In this design procedure, the backbone from 4m5.3 is modeled as the starting structure in all regions except HCDR3, and the entire HCDR3 backbone is replaced with the one observed in each

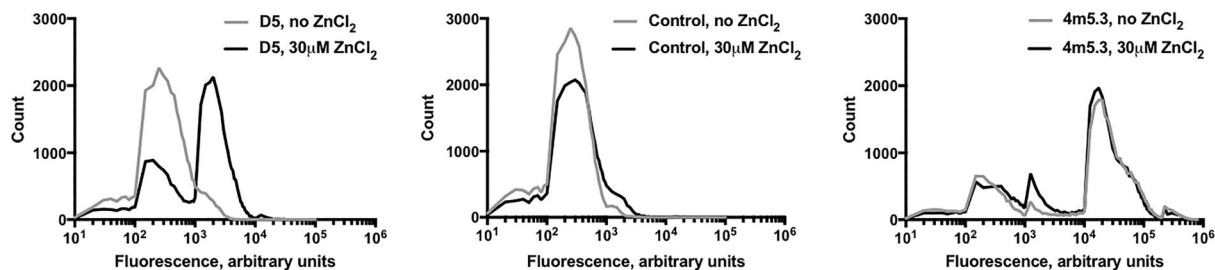


**Figure 2.** Fluorescein binding by design D5 is positively regulated by  $Zn^{2+}$ . Flow cytometric analysis of yeast cells expressing (from left-to-right): D5, antibody 4m5.3, and an unrelated negative control. Fluorescein binding in the absence (gray) and presence of  $30\mu M ZnCl_2$  (black) was probed by labeling with biotinylated fluorescein conjugated to streptavidin-APC. Shown are the histograms of FL4 (APC) signal. Display levels were not affected by  $ZnCl_2$  [Supporting Information Fig. S3(A)].

of the alternative antibodies. Following backbone design, Rosetta calculations are used to optimize the amino acid sequence within  $8\text{\AA}$  of the designed HCDR3 using the Rosetta all-atom energy function, which is dominated by contributions from van der Waals packing, hydrogen bonding, electrostatics, and solvation. Following design, we eliminated models, in which the new HCDR3 sterically overlapped with fluorescein in the binding mode observed in PDB entry 1X9Q, and used RosettaMatch<sup>22</sup> to design  $Zn^{2+}$ -coordinating residues in and around the designed HCDR3.<sup>23</sup> Our designs implemented tetrahedral  $Zn^{2+}$ -coordination sites using several three-residue constellations, including three-His sites (HHH), and two His and one Asp or Glu sites (DHH or EHH, respectively); the fourth coordination site was left open for water without explicit modeling, and we visually verified that the fourth site resided in bulk solvent in all designs. HHH, DHH, and EHH constellations are the most prevalent tetrahedral coordination architectures for  $Zn^{2+}$  in nature,<sup>24</sup> and we therefore did not attempt to design constellations comprising two or more acidic sidechains. Following the design of  $Zn^{2+}$ -coordinating residues, the sequence and sidechain conformations of residues within  $8\text{\AA}$  of  $Zn^{2+}$  were optimized by RosettaDesign<sup>25</sup> using the all-atom energy function, and the resulting structure models were filtered according to computed fluorescein-binding energy and the designs' closeness to ideal tetrahedral  $Zn^{2+}$ -coordination geometry. This design procedure therefore aimed to incorporate a  $Zn^{2+}$ -coordination site, which did not overlap with the native fluorescein-binding site, while minimizing the expected decrease in the design's stability and fluorescein-binding affinity relative to 4m5.3.

We tested 71 designs that passed our structure and energy filters using yeast cell surface display (Supporting Information Table SI).<sup>26</sup> Genes encoding the antibodies were formatted as single-chain variable fragments (scFv), cloned into the pETCON yeast display vector,<sup>27</sup> and used to transform yeast EBY100 cells. About 60 of the 71 designs showed medium-to-high surface-expression levels (defined as

>30% of the levels observed for 4m5.3). Eight designs, which were based on five different HCDR3 template backbones, bound a fluorescein probe [Supporting Information Table SIII, Supporting Figs. 1 and 3(A)]; two of the templates came from fluorescein-binding antibodies, and the other three from catalytic antibodies. Of the eight fluorescein-binding designs, design 5 (D5) exhibited the desired activity profile, and showed no detectable binding to the fluorescein probe in the absence of  $Zn^{2+}$ , whereas fluorescein binding to antibody 4m5.3 showed no dependence on  $Zn^{2+}$  (Fig. 2). We also noted that D5's expression levels were <50% those of 4m5.3, indicating reduced stability.<sup>28</sup>

Because fluorescein binding quenches its fluorescence, the probe used in our yeast-display experiments was biotinylated fluorescein conjugated to the fluorescent streptavidin-APC.<sup>29</sup> To verify that the binding signal observed in these experiments was due to fluorescein and not to the much larger streptavidin-APC moiety, we next tested D5 binding to biotinylated fluorescein in the presence and absence of  $Zn^{2+}$ . D5 scFv was expressed in *E. coli* BL21 cells, isolated from inclusion bodies, refolded, and seen to be mostly monomeric on size-exclusion chromatography (>80%; Supporting Information Fig. S2). We then measured binding to biotinylated fluorescein by surface-plasmon resonance. The apparent  $K_D$  in the absence of  $Zn^{2+}$  was nearly tenfold higher than in its presence ( $3.2\ \mu M$  and  $0.4\ \mu M$ , respectively), and the response to fluorescein was 2- to 4-fold higher (depending on fluorescein concentration) in the presence of  $50\ \mu M Zn^{2+}$  than in its absence (Fig. 3, Supporting Information Table SIV). Furthermore, binding kinetic measurements showed that the increase in affinity was due to a faster on-rate in the presence of  $Zn^{2+}$  ( $8.06 \times 10^4\ M^{-1}\ s^{-1}$  and  $4.16 \times 10^3\ M^{-1}\ s^{-1}$ , respectively), suggesting that the application of  $Zn^{2+}$  preorganized the Fv for fluorescein binding. We therefore concluded that fluorescein binding by D5 was indeed positively regulated by  $Zn^{2+}$ , and that this regulation came at the cost of reduced stability and six orders of magnitude lower fluorescein affinity relative to 4m5.3. Despite

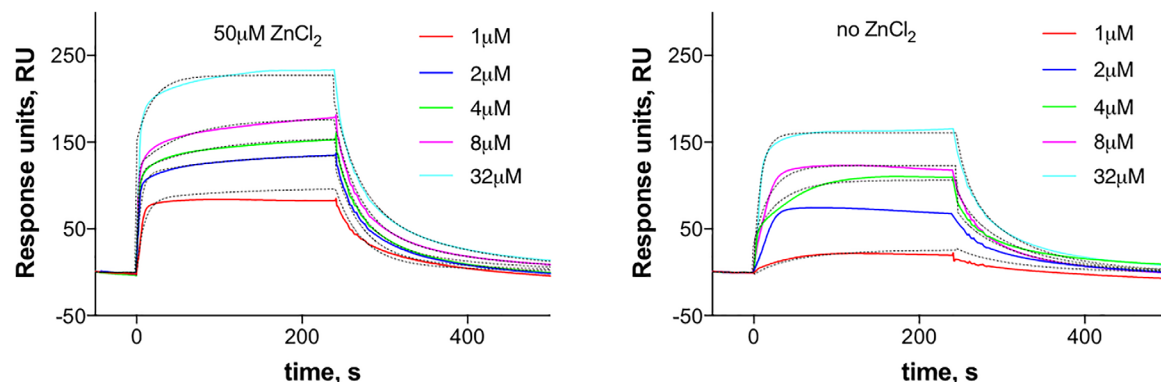


**Figure 3.** D5 shows higher affinity and higher response levels to fluorescein in the presence of  $Zn^{2+}$ . Surface-plasmon resonance analysis of design D5 in the presence of  $Zn^{2+}$  (left) and in its absence (right). The data were fitted to a model of heterogeneous ligand with parallel reactions, and the fits are shown as black dashed lines. The apparent  $K_D$  is 0.4 and  $3.2\mu M$ , respectively, and kinetic fits show that most of the difference is due to faster on-rates in the presence of  $Zn^{2+}$  (Supporting Information Table SIV).

our attempts, more detailed analysis of D5 binding to fluorescein in solution could not be carried out, since the protein precipitates at high concentrations (including when tested as Fab or IgG).

D5's HCDR3 backbone conformation was based on an intermediate-affinity fluorescein-binding antibody (PDB entry: 1T66;  $K_D = 27nM$ ), which was, however, not the evolutionary ancestor of 4m5.3, and had a different HCDR3 conformation from 4m5.3. D5's computed fluorescein-binding energy was among the best among our models ( $-17$  Rosetta energy units) indicating that this design was particularly well-suited to  $Zn^{2+}$ -coordination and fluorescein binding. Two of D5's  $Zn^{2+}$ -coordinating histidines were located in HCDR3, and the third was in HCDR1 [Fig. 1(B)]. To test whether D5's activation by  $Zn^{2+}$  depended on the designed  $Zn^{2+}$ -binding site, we analyzed binding by mutants in and around the chelating residues [Fig. 4(A) and Supporting Information Fig. S3(B)] using yeast display. Single-point mutations His<sup>H99</sup>Gly and His<sup>H102</sup>Tyr (following Kabat numbering<sup>17</sup>), which reverted  $Zn^{2+}$ -coordinating positions to their identities in PDB entry

1T66, significantly reduced fluorescein binding in the presence of  $Zn^{2+}$ . By contrast, the conservative mutations His<sup>H27</sup>Phe and Gly<sup>H96</sup>Ser increased fluorescein binding, but the positive regulation by  $Zn^{2+}$  was lost. These results indicated that D5 was highly sensitive to the molecular details in the region surrounding the designed HCDR3, and its sensitivity to  $Zn^{2+}$  came at the cost of reduced fluorescein binding relative even to conservative point mutations.

We next tested D5's sensitivity to the effector ion's identity by replacing  $Zn^{2+}$  with other divalent metal ions and measuring fluorescein binding using yeast display [Fig. 4(B) and Supporting Information Fig. S4]. At  $30\mu M$  concentration, all divalent ions activated D5 to some extent; the fluorescein-binding response to  $Zn^{2+}$ , however, was nearly twice as high as to any of the other ions. The most significant response we saw for an ion other than  $Zn^{2+}$  was due to  $Cu^{2+}$  (60% of the  $Zn^{2+}$  response), which is indeed the most similar divalent ion to  $Zn^{2+}$  in terms of atomic radius and coordination geometry.<sup>30</sup> Hence, the design requirements, introducing an allosteric site that would be preconfigured only in the presence

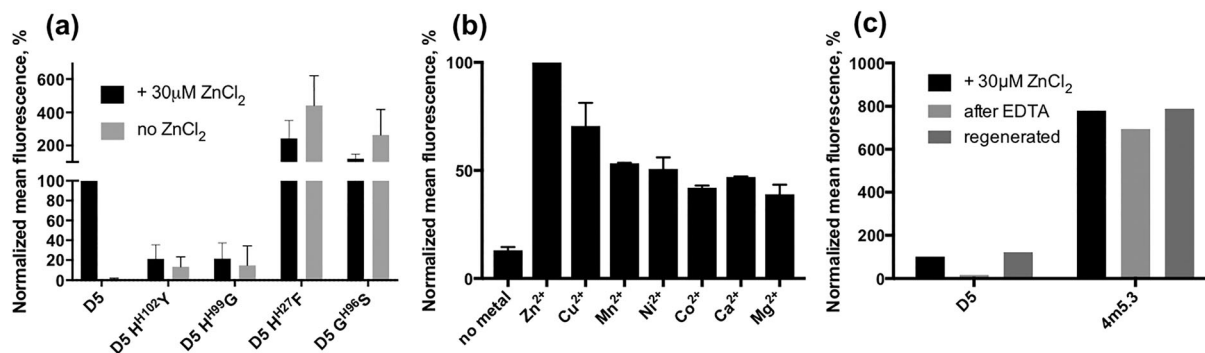


**Figure 4.** D5 regulation by  $Zn^{2+}$  is fully reversible and is sensitive to conservative point mutations and type of divalent ion. Shown is mean fluorescence data from two independent yeast-display experiments, normalized to fluorescence of D5 in the presence of  $30\mu M Zn^{2+}$ . A. Effect of mutations on fluorescein binding of design D5. Some mutants reduce  $Zn^{2+}$  sensitivity and others reduce fluorescein binding. B. Metal-binding specificity. C. Regeneration of  $Zn^{2+}$  binding after stripping by the metal-chelator EDTA.

of Zn<sup>2+</sup> are very stringent, but D5 nevertheless met these requirements and additionally exhibited selectivity for Zn<sup>2+</sup> over other divalent ions, depending on their size and coordination geometry.

Natural allosteric proteins are reversibly activated and deactivated, and we found that Zn<sup>2+</sup> binding by D5 was also reversible [Fig. 4(C)]: after stripping Zn<sup>2+</sup> by incubation with the metal-chelator EDTA, fluorescein binding was lost, but was fully restored by washing and repeated application of Zn<sup>2+</sup>. The design therefore has some of the selectivity, sensitivity, and reversibility hallmarks of natural molecular sensors.

## Discussion

We designed a sensitive and reversible allosteric regulation site in an antibody variable domain by optimizing HCDR3 and surrounding residues for Zn<sup>2+</sup> coordination. The design of allosteric regulation demands control over multiple protein states, a challenge that has only been addressed in a few cases.<sup>31,32</sup> Here, instead, we explicitly designed only the target ligand- and effector-bound state and predicted that the effector-unbound state would be flexible, thereby reducing its affinity for the ligand. Although successful, the designed allosteric site came at the cost of reduced stability and lower affinity for the ligand fluorescein; it is also noteworthy that we only obtained one design with the desired activity profile from 71 tested, further emphasizing the challenge of balancing the conflicting requirements of protein flexibility, stability, and binding. We speculate that natural allosteric proteins might have emerged from non-allosteric binding proteins through similar intermediates, in which effector responsiveness came at a cost to stability, ligand-affinity, or both. D5 may therefore serve to investigate the emergence of allosteric regulation from non-allosteric binding proteins during evolution. The mutation analysis reported above, however, demonstrates D5's extreme sensitivity to conservative point mutations, whereas many natural allosteric proteins show remarkable plasticity and an ability to change regulatory characteristics through evolution.<sup>33</sup> D5's relative intolerance to mutation may stem from the fact that the designed allosteric site is spatially closer to the substrate-binding site than often seen in natural proteins. Finally, we note that given the ubiquity of antibodies in research, the design algorithm may provide a way to rational design of sensitive and regulated molecular sensors.

## Materials and Methods

### Design

*AbDesign*<sup>21</sup> was used to construct a conformation database for HCDR3 backbones and to model these backbones into the 4m5.3 template scaffold (PDB ID: 1X9Q), followed by sequence optimization in and around HCDR3. RosettaMatch<sup>22</sup> was used to place

the tetrahedral Zn<sup>2+</sup>-coordination site into the designed antibodies. The sequence was subsequently optimized with EnzDes<sup>25</sup> using five cycles of design and filtering the designs by the geometry of Zn<sup>2+</sup>-coordinating residues (constraints) and fluorescein-binding energy (ligand interface energy and repulsion energy). RosettaScripts<sup>34</sup> design protocols and full details of the design process are given in the Supporting Information.

### Gene synthesis, cloning, and mutagenesis

The genes of the 71 designed scFvs (14, 23, and 34 designs with HHH, DHH, and EHH-coordination geometry, respectively) were synthesized by Gen9, Inc. (Cambridge, MA) and cloned into the pETCON vector by homologous recombination upon transformation into yeast.<sup>35</sup> The gene of design D5 for bacterial expression was ordered from Genscript (Piscataway, NJ) in pET29b vector. Point mutations were introduced by QuickChange protocol<sup>36</sup> (Supporting Information Table SII). The gene encoding design D5 will be deposited upon publication in AddGene.

### Yeast surface display

Designed proteins were tested for fluorescein binding in the presence and absence of Zn<sup>2+</sup> using yeast surface display.<sup>26</sup> Yeast surface protein expression was monitored by binding of anti-c-Myc Alexa Fluor647 antibody (Santa Cruz Biotechnology) to the C-terminal c-Myc tag of the displayed scFv. Cells were washed with Hepes solution (50 mM Hepes, pH 7.5), incubated for 0.5 h/4°C with solution of anti-c-Myc Alexa Fluor647 (2 μg mL<sup>-1</sup> in Hepes with 0.1% BSA), and washed twice with ice-cold Hepes. Fluorescein binding was assessed by incubation with 1 μM fluorescein-biotin conjugate (AnaSpec Inc., Fremont, CA), followed by incubation with streptavidin-APC (Southern Biotech). Cells were washed with Hepes solution, incubated for 0.5 h at room temperature with 1 μM fluorescein-biotin in Hepes, washed with ice cold Hepes, incubated for 20 min/4°C with streptavidin-APC (0.01 mg mL<sup>-1</sup> in Hepes with 0.1% BSA), and then washed twice with ice cold Hepes. Cellular fluorescence was monitored on an Accuri C6 flow cytometer using filter FL4. We noted non-specific binding to yeast cells with fluorescein-biotin concentrations >10 μM.

In the samples with Zn<sup>2+</sup>, all the solutions, including growth medium, contained 30 μM ZnCl<sub>2</sub> (we noted that ZnCl<sub>2</sub> concentrations >100 μM were toxic to yeast cells, and caused reduced binding signals and cell clumping). In the samples without Zn<sup>2+</sup>, no ZnCl<sub>2</sub> was added, and in the initial washing step, the cells were washed with Hepes solution supplemented with 10 mM EDTA. An unrelated antibody available in our laboratory<sup>37</sup> was used as a negative control in yeast display experiments.

### **Metal stripping and replacement**

Divalent ions were stripped from design D5 by incubation of yeast cells with 1mM EDTA (1 h at room temperature), and the cells were tested for fluorescein binding. The cells were then washed, reincubated with 30 $\mu$ M of ZnCl<sub>2</sub>/MgCl<sub>2</sub>/CaCl<sub>2</sub>/NiCl<sub>2</sub>/MnSO<sub>4</sub>/CoSO<sub>4</sub>/CuSO<sub>4</sub> (0.5 h at room temperature) and tested for fluorescein binding as previously described, while keeping the ions in all the solutions.

### **D5 scFv expression and purification from inclusion bodies**

The scFvs were produced essentially as described,<sup>38</sup> with EDTA omitted in all the steps.

### **Surface plasmon resonance (SPR)**

SPR experiments were carried out using BIAcore T200 (GE Healthcare). Experiments were performed at 25°C in 10 mM HEPES pH 7.4, 150 mM NaCl, and 0.005% Tween 20 (running buffer). Design D5 was immobilized on a CM5 chip (GE Healthcare) by amine coupling to a total of roughly 5,000 response units (RU). Running buffer with 50  $\mu$ M ZnCl<sub>2</sub> was injected for 1,800 s at 2  $\mu$ L min<sup>-1</sup>, and then for 600 s before each injection of analyte. A concentration series of biotinylated fluorescein (1, 2, 4, 8, and 32  $\mu$ M in running buffer) was injected over the coated chip for 240s at 10  $\mu$ L min<sup>-1</sup>, followed by 600-s dissociation. In the experiment without Zn<sup>2+</sup>, running buffer with 1mM EDTA was injected for 1,800s at 2  $\mu$ L min<sup>-1</sup>, before analyte injections. Specific binding was obtained by subtracting the response of a blank surface from that of the surface coated by design D5. The data were analyzed using BIAevaluation 4.1.1 software and fitted to the heterogeneous ligand with parallel reactions model. The data from flowing 2  $\mu$ M analyte without Zn<sup>2+</sup> were excluded from parameter fitting for inconsistency with the other traces, but are shown in Figure 3 for completeness.

### **Acknowledgment**

The authors thank Gideon Lapidoth for assistance in design calculations and Gideon Schreiber for assistance in SPR analysis and for critical reading.

### **References**

1. Monod J, Changeux J-P, Jacob F (1963) Allosteric proteins and cellular control systems. *J Mol Biol* 6:306–329.
2. Tsai CJ, Nussinov R (2014) A unified view of “how allostery works.” *PLoS Comput Biol* 10:e1003394.
3. Motlagh HN, Wrabl JO, Li J, Hilser VJ (2014) The ensemble nature of allostery. *Nature* 508:331–339.
4. Makhlynets OV, Raymond EA, Korendovych IV (2015) Design of allosterically regulated protein catalysts. *Biochemistry* 54:1444–1456.
5. Kanwar M, Wright RC, Date A, Tullman J, Ostermeier M (2013) Protein switch engineering by domain insertion. *Methods Enzymol* 523:369–388.
6. Lee J, Natarajan M, Nashine VC, Socolich M, Vo T, Russ WP, Benkovic SJ, Ranganathan R (2008) Surface sites for engineering allosteric control in proteins. *Science* 322:438–442.
7. Reynolds KA, McLaughlin RN, Ranganathan R (2011) Hot spots for allosteric regulation on protein surfaces. *Cell* 147:1564–1575.
8. Liang J, Kim JR, Boock JT, Mansell TJ, Ostermeier M (2007) Ligand binding and allostery can emerge simultaneously. *Protein Sci* 16:929–937.
9. Korendovych IV, Kulp DW, Wu Y, Cheng H, Roder H, DeGrado WF (2011) Design of a switchable eliminase. *Proc Natl Acad Sci USA* 108:6823–6827.
10. Moroz YS, Dunston TT, Makhlynets OV, Moroz OV, Wu Y, Yoon JH, Olsen AB, McLaughlin JM, Mack KL, Gosavi PM, van Nuland NA, Korendovych IV. (2015) New tricks for old proteins: single mutations in a non-enzymatic protein give rise to various enzymatic activities. *J Am Chem Soc* 137:14905–14911.
11. Raymond EA, Mack KL, Yoon JH, Moroz OV, Moroz YS, Korendovych IV (2015) Design of an allosterically regulated retroaldolase. *Protein Sci* 24:561–570.
12. Taylor ND, Garruss AS, Moretti R, Chan S, Arbing M, Cascio D, Rogers JK, Isaacs FJ, Kosuri S, Baker D, Fields S, Church GM, Raman S. (2016) Engineering an allosteric transcription factor to respond to new ligands. *Nat Methods* 13:177–183.
13. Williams DM, Wang D, Cole PA (2000) Chemical rescue of a mutant protein-tyrosine kinase. *J Biol Chem* 275:38127–38130.
14. Xia Y, Diprimio N, Keppel TR, Vo B, Fraser K, Battaile KP, Egan C, Bystruff C, Lovell S, Weis DD, Anderson C, Karanicolas J. (2013) The designability of protein switches by chemical rescue of structure: mechanisms of inactivation and reactivation. *J Am Chem Soc* 135:18840–18849.
15. Fleishman SJ, Baker D (2012) Role of the biomolecular energy gap in protein design, structure, and evolution. *Cell* 149:262–273.
16. Midelfort KS, Hernandez HH, Lippow SM, Tidor B, Drennan CL, Witttrup KD (2004) Substantial energetic improvement with minimal structural perturbation in a high affinity mutant antibody. *J Mol Biol* 343:685–701.
17. Wu TT, Kabat EA (1970) An analysis of the sequences of the variable regions of Bence Jones proteins and myeloma light chains and their implications for antibody complementarity. *J Exp Med* 132:211–250.
18. Warszawski S, Netzer R, Tawfik DS, Fleishman SJ (2014) A “fuzzy”-logic language for encoding multiple physical traits in biomolecules. *J Mol Biol* 426:4125–4138.
19. Ollikainen N, Smith CA, Fraser JS, Kortemme T (2013) Flexible backbone sampling methods to model and design protein alternative conformations. *Methods Enzymol* 523:61–85.
20. Finn BE, Evenas J, Drakenberg T, Waltho JP, Thulin E, Forsen S (1995) Calcium-induced structural changes and domain autonomy in calmodulin. *Nat Struct Biol* 2:777–783.
21. Lapidoth GD, Baran D, Pszolla GM, Norn C, Alon A, Tyka MD, Fleishman SJ (2015) AbDesign: an algorithm for combinatorial backbone design guided by natural conformations and sequences. *Proteins* 83:1385–1406.
22. Zanghellini A, Jiang L, Wollacott AM, Cheng G, Meiler J, Althoff EA, Röthlisberger D, Baker D (2006) New algorithms and an in silico benchmark for computational enzyme design. *Protein Sci* 15:2785–2794.
23. Der BS, MacHius M, Miley MJ, Mills JL, Szyperski T, Kuhlman B (2012) Metal-mediated affinity and

- orientation specificity in a computationally designed protein homodimer. *J Am Chem Soc* 134:375–385.
24. Alberts IL, Nadassy K, Wodak SJ (1998) Analysis of zinc binding sites in protein crystal structures. *Protein Sci* 7:1700–1716.
  25. Richter F, Leaver-Fay A, Khare SD, Bjelic S, Baker D (2011) De novo enzyme design using Rosetta3. *PLoS One* 6:e19230.
  26. Chao G, Lau WL, Hackel BJ, Sazinsky SL, Lippow SM, Wittrup KD (2006) Isolating and engineering human antibodies using yeast surface display. *Nat Protoc* 1:755–768.
  27. Fleishman SJ, Whitehead TA, Ekiert DC, Dreyfus C, Corn JE, Strauch E-M, Wilson IA, Baker D (2011) Computational design of proteins targeting the conserved stem region of influenza hemagglutinin. *Science* 332:816–821.
  28. Shusta EV, Kieke MC, Parke E, Kranz DM, Wittrup KD (1999) Yeast polypeptide fusion surface display levels predict thermal stability and soluble secretion efficiency. *J Mol Biol* 292:949–956.
  29. Boder ET, Wittrup KD (2000) Yeast surface display for directed evolution of protein expression, affinity, and stability. *Methods Enzymol* 328:430–444.
  30. Lippard SJ, Berg J (1994) *Principles of bioinorganic chemistry*. University Science Books, Mill Valley, California.
  31. Hoersch D, Roh S, Chiu W, Kortemme T (2013) Reprogramming an ATP-driven protein machine into a light-gated nanocage. *Nat Nanotechnol* 8:928–932.
  32. Joh NH, Wang T, Bhate MP, Acharya R, Wu Y, Grabe M, Hong M, Grigoryan G, DeGrado WF (2014) De novo design of a transmembrane Zn<sup>2+</sup>-transporting four-helix bundle. *Science* 346:1520–1524.
  33. Komiyama NH, Miyazaki G, Tame J, Nagai K (1995) Transplanting a unique allosteric effect from crocodile into human haemoglobin. *Nature* 373:244–246.
  34. Fleishman SJ, Leaver-Fay A, Corn JE, Strauch EM, Khare SD, Koga N, Ashworth J, Murphy P, Richter F, Lemmon G, Meiler J, Baker D. (2011) Rosettascripts: a scripting language interface to the Rosetta macromolecular modeling suite. *PLoS One* 6:e20161.
  35. Gietz RD, Schiestl RH (2007) Quick and easy yeast transformation using the LiAc/SS carrier DNA/PEG method. *Nat Protoc* 2:35–37.
  36. Braman J, Papworth C, Greener A (1996) Site-directed mutagenesis using double-stranded plasmid DNA templates. *Methods Mol Biol* 57:31–44.
  37. Grossman I, Alon A, Ilani T, Fass D (2013) An inhibitory antibody blocks the first step in the dithiol/disulfide relay mechanism of the enzyme QSOX1. *J Mol Biol* 425:4366–4378.
  38. Buchner J, Pastan I, Brinkmann U (1992) A method for increasing the yield of properly folded recombinant fusion proteins: single-chain immunotoxins from renaturation of bacterial inclusion bodies. *Anal Biochem* 205:263–270.